Evaluating Three Evapotranspiration Mapping Algorithms with Lysimetric Data in the Semi-arid Texas High Plains

José L. Chávez[1,2], Prasanna H. Gowda[2], Terry A. Howell[2], and Karen S. Copeland[2]

Conservation and Production Research Laboratory
USDA-Agricultural Research Service
P.O. Drawer 10
Bushland, TX 79012-0010

Abstract

Ground water levels are declining at unsustainable rates in the Texas High Plains. Accurate evapotranspiration (ET) maps would provide valuable information on regional crop water use and hydrology. This study evaluated three remote sensing based algorithms for estimating ET rates for the Texas High Plains. Data from four large-scale weighing lysimeters (two each irrigated and dryland crops) at the Conservation Production Research Laboratory, USDA-ARS at Bushland, TX, were used to evaluate the remote sensing methods. ET algorithms evaluated include Mapping Evapotranspiration at High Resolution using Internalized Calibration model (METRIC), Two-Source Energy Balance model (TSM), and an Aerodynamic Temperature based Energy Balance model (ATEB). A Landsat 5 TM image acquired on July 23, 2006 was used for estimating ET. Predicted ET values were compared with lysimetric data to determine how well the different ET models worked. A discussion of each model's strength and weaknesses, under the climatic conditions encountered in the Texas High Plains, is provided.

Keywords: Texas Panhandle, semi-arid environment, remote sensing, irrigation scheduling, surface energy balance.

Introduction

The Ogallala Aquifer is the main source of water supply for the Texas High Plains (THP) and is being depleted at an unsustainable rate (Axtell, 2006). In the THP, irrigation alone uses approximately 89% of the water pumped from the Ogallala Aquifer (Dennehy, 2000). McGuire (2004) indicated that the change in water storage in the aquifer beneath the THP, from predevelopment to 2003, was about 164.1 km^3 (5.2 km^3 from 2002 to 2003) with an average area-weighted predevelopment water-level decline of 10.6 m

[1] Corresponding author, email: jchavez@cprl.ars.usda.gov
[2] Agricultural Engineer, Agricultural Engineer, Agricultural Engineer and Research Leader, and Soil Scientist, respectively.

(0.37 m from 2002 to 2003). For this reason and considering the positive trends in population growth in the THP, there is a need for greater efficiency in irrigation water management for agriculture.

Improvement in irrigation water management is achieved when the beneficial crop water use is accurately quantified in time and space. Remote sensing (RS) based evapotranspiration (ET) methods are found to be useful for deriving such information. Numerous RS algorithms, such as METRIC (Mapping Evapotranspiration at high Resolution with Internal Calibration; Allen et al., 2007, 2005a), SEBAL (Surface Energy Balance for Land; Bastiaanssen et al., 1998), a Two-Source energy balance Model (TSM; Norman et al., 1995), Aerodynamic Temperature based energy balance models [Chávez et al., 2005; Crago et al. (1999), Crago (1998), and Chehbouni et al. (1996, 1997)], a dimensionless temperature method (Δ_T, Suleiman and Crago, 2004), and an Analytical Land Atmosphere Radiometer Model (ALARM; Suleiman and Crago, 2002), among others, have been developed to spatially estimate crop water consumption or ET and are being evaluated around the world. These algorithms mainly solve the energy balance of the land surface for latent heat flux (LE) at the time of satellite or airborne RS system overpass and extrapolate instantaneous LE (ET_i) to daily ET values.

Gowda et al. (2007a) discussed the pros and cons of numerous RS algorithms for ET estimation. For instance, they indicated that the TSM model yielded surface heat fluxes with errors within 10-12%, although this model demands several crop and micro-meteorological data that, in many circumstances, are very difficult to obtain. They summarized that SEBAL had a typical accuracy at the field scale of 85 % or errors ranging from 2.7 to 35.0 % with an overall average of 18.2 %, under a variety of climatic/environmental conditions. However, METRIC appeared to have an advantage over SEBAL under advective conditions. METRIC's ET estimation errors were reported to be approximately 10 to 20 % for daily estimates and as low as 1 to 4 % for seasonal ET estimates, requiring only vapor pressure (or relative humidity) and wind speed measurements from weather stations (WS) within the satellite scene. METRIC, as in SEBAL, needs to be applied by individuals with background knowledge in hydrology, engineering, and environmental physics, and demands experience in the selection process of the cold/wet and hot/dry pixels in the remote sensing scene in order to properly determine a relationship between surface radiometric temperature and dT (aerodynamic temperature – air temperature) for estimating sensible heat fluxes. The need of extreme pixel selection does not apply for aerodynamic temperature based land surface energy balance algorithms. Therefore, in this study, three distinct methods have been selected to assess their ability to accurately predict spatial ET in the THP: METRIC (based on extreme pixels); TSM (based on the discrimination of canopy and soil temperature); and the Aerodynamic Temperature based Energy Balance method by Chávez et al. (2005), herein denominated ATEB, which is a function of radiometric surface temperature, air temperature, leaf area index, and wind speed.

Materials and Methods

Study Area

This study was conducted at the USDA-ARS, Conservation and Production Research Laboratory (CPRL), located in Bushland, Texas, USA (Fig. 1). The geographic coordinates of the CPRL are 35° 11' N, 102° 06' W, and its elevation is 1,170 m above mean sea level. For this study, a 30-m resolution Landsat 5 Thematic Mapper (TM) scene was used to derive energy fluxes at the land surface. The scene path/row was 31/36 and was acquired at 11:20 CST (17:20 GMT) on July 23, 2006. Thermal band (TM band 6) image was captured at a coarser resolution of 120-m, and was resampled to 30–m by the image supplier. Soils around Bushland are classified as slowly permeable Pullman clay loam soils. The major crops in the region are corn, sorghum, winter wheat and cotton.

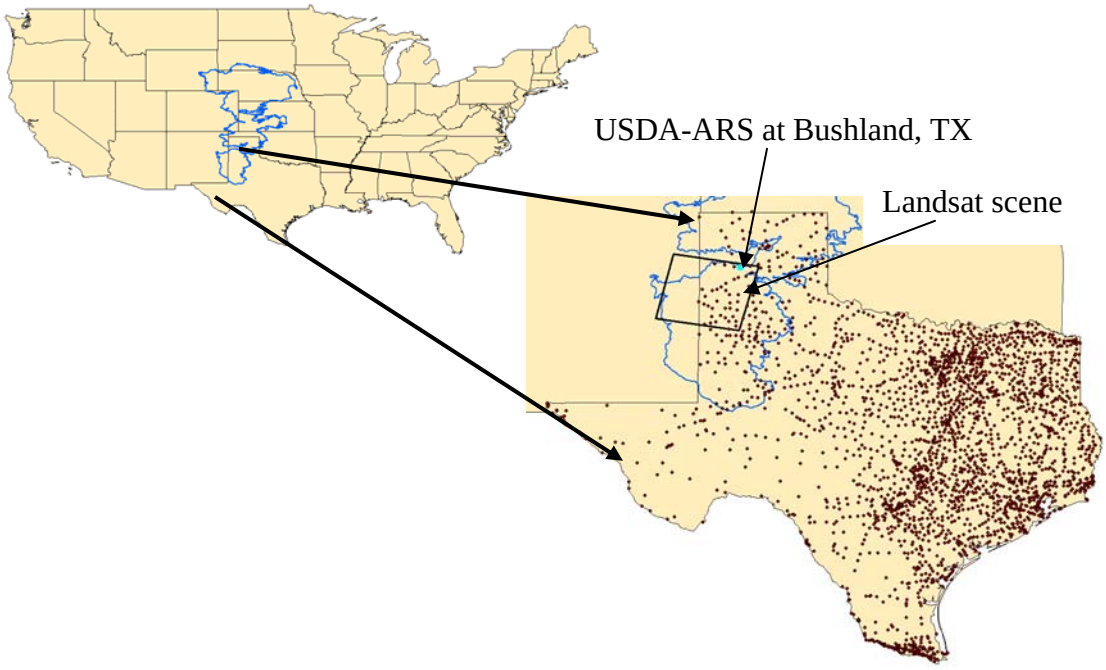

Figure 1. Landsat 5 TM path/row 31/36 scene (rectangle) covering an area underlaid by the Ogallala Aquifer (irregular polygon) in the Texas High Plains (Panhandle). The USDA-ARS-CPRL laboratory location is indicated by a dot.

Estimated ET values were verified by comparing them with soil water mass change-based daily ET values from five monolithic weighing lysimeters located at the CPRL (Fig. 2). Four large lysimeters (3 m length x 3 m width x 2.5 m depth) were located in the middle of 4.7-ha fields. In 2006, the SW and NW lysimeters were planted to dryland grain sorghum with NW field planted in clumps as part of another study. The irrigated SE and NE lysimeter fields were planted to forage sorghum and corn, respectively. The grass lysimeter was 1.5 m by 1.5 m by 2.5 m deep and was located in

the reference ET weather station field (0.31 ha) which is a part of the Texas High Plains ET Network (TXHPET, 2006). Each lysimeter field is equipped with one net radiometer [Q*7.1, Radiation and Energy Balance Systems (REBS) [3/], Seattle, WA] and one infra-red thermometer (IRT) (2G-T-80F/27C, Exergen, Watertown, MA) for measuring net radiation and surface temperature, respectively.

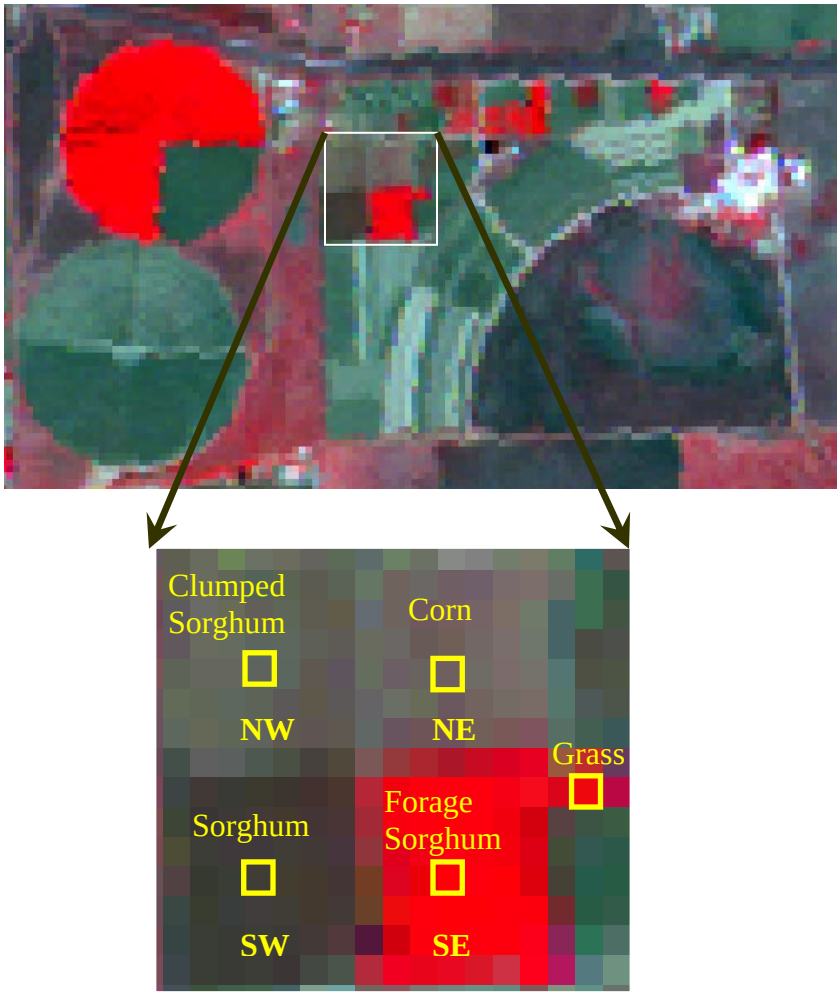

Figure 2. Landsat 5 TM false color image showing lysimeter locations at USDA-ARS-CPRL facility in Bushland, TX.

[3/] Mention of trade names or commercial products in this publication is solely for the purpose of providing specific information and does not imply recommendation or endorsement by the United States Department of Agriculture.

Lysimeter Setup

Each of the four large lysimeters at Bushland contains monolithic Pullman clay loam soil core. Change in the soil water mass is used for determining ET values. Changes in lysimeters mass were determined using a data logger (model CR7-X, Campbell Scientific, Inc., Logan, UT) to measure and record the lysimeter load cell (model SM-50, Interface, Scottsdale, AZ) with the signal sampled at 0.17-Hz (every 6 s) frequency. The lysimeters calibration can be found in Howell et al. (1995). The lysimeter mass measurement accuracy in water depth equivalent was 0.01 mm, as indicated by the root mean squared error of calibration. The load cell signal was averaged for 5 min and composited to 60-min means. The lysimeter mass data were reported on the midpoint of the 60 min, that is, data were averaged from 0 to 60 min and reported at the midpoint of the averaging period. Daily ET was calculated as the difference between lysimeters mass recorded at 2330 h CST of one day and 2330 h CST of the next day to determine mass losses (from evaporation and transpiration) to which lysimeter mass gains (from irrigation or precipitation) were added. A vacuum pump regulated to -10 kPa provided drainage, and the drainage effluent was held in two tanks suspended from the lysimeters and weighed with lever-load cells.

Radiometric and atmospheric calibration of Satellite data

Landsat 5 TM imagery was obtained as digital numbers (DN) which were first converted into radiance (L_b), for each band as L_b= (gain x DN) + bias), then 'at sensor' or 'Top-of-the-Atmosphere' (TOA; exoatmospheric) reflectance values for the shortwave bands were estimated. Reflectance values were calculated by dividing the detected radiance at the satellite (for each band) by the incoming energy (radiance) in the same shortwave band. The incoming radiance is a function of mean solar exoatmospheric irradiance, solar incidence angle, and the inverse square of the relative earth-to-sun distance. In the case of the thermal band, the spectral radiance values were converted into effective at-satellite temperatures of the viewed earth-atmosphere system under an assumption of unity for surface emissivity and using pre-launch calibration constants by means of an inverted logarithmic formula. Detailed steps on the Landsat 5 TM radiometric calibration procedures can be found in Chander and Markham (2003). Subsequently, surface reflectance values were computed after applying atmospheric interference corrections, on the TOA reflectance image, for shortwave absorption and scattering using narrowband transmittance values for each band as calibrated by Tasumi et al. (2005) for METRIC; which obtains surface temperature after correcting the at-satellite effective 'brightness' temperatures for surface emissivity only. However, images were calibrated using MODTRAN v4 (Berk et al., 2000) for TSM and ATEB. With the MODTRAN procedure, thermal surface emissivity and atmospheric interference were accounted.

Remote Sensing based ET Algorithms

In this section, TSM, METRIC, and ATEB are described. Several sub-models are common in all and are described without specifying the name of the EB algorithm. However, we indicate model denomination where the EB sub-models are different.

In all three algorithms, ET is computed as a residual from the surface energy balance equation as an instantaneous ET or latent heat flux (LE) [Note: ET = LE ρ_w^{-1} λ_{LE}^{-1}, where ET is in mm d^{-1}, LE is in MJ m^{-2} d^{-1}, ρ_w is water density in Mg m^{-3} (~1.0 Mg m^{-3}), and λ_{LE} is the latent heat of vaporization in MJ kg^{-1} (~2.45 MJ kg^{-1})] for the time of the satellite overpass, as shown in Eqn. (1).

$$LE = R_n - G - H \tag{1}$$

where, R_n is net radiation (W m^{-2}), G is the soil heat flux (W m^{-2}) and H is the sensible heat flux (W m^{-2}). LE is converted to ET (mm h^{-1} or mm d^{-1}) by dividing it by the latent heat of vaporization (λ_{LE}; ~2.45 MJ kg^{-1}), density of water (ρ_w; ~1.0 Mg m^{-3}), and an appropriate time constant [Note: 1 W = 1 J s^{-1}]. The sign convention for the different flux terms in Eqn. (1) is positive from the land surface to the atmosphere (up) for LE and H, and positive towards the surface for R_n and into the ground (down) for G. R_n is calculated using surface reflectance and surface radiometric temperature (T_s) derived from satellite imagery, near surface vapor pressure from a near-by weather station (WS), and R_s as explained below. R_n is the result of the surface energy budget between short and long wave radiation terms [Eqn. (2) for METRIC, and Eqn. (3) for TSM and ATEB].

$$R_n = R_s\downarrow - \alpha R_s\downarrow + R_L\downarrow - R_L\uparrow - (1-\varepsilon_o)R_L\downarrow \tag{2}$$

$$R_n = (1-\alpha)R_s\downarrow + R_L\downarrow - R_L\uparrow \tag{3}$$

where, $R_s\downarrow$ is incoming shortwave radiation (W m^{-2}). $R_s\downarrow$ was measured with a pyranometer (model CMP 6, Kipp and Zonen, Bohemia, NY) installed at the ARS-Bushland weather station (TXHPET, 2006). Surface albedo (α) is a function of surface reflectance values in the shortwave portion of the electro-magnetic spectrum (a weighted average of reflectance in TM bands 1, 2, 3, 4, 5 and 7 for METRIC, and of bands 3 and 4 for TSM and ATEB; Brest and Goward, 1987), dimensionless; $R_L\downarrow$ is incoming long wave radiation (W m^{-2}) or downward thermal radiation flux originated from the atmosphere which was estimated using the Stefan-Boltzmann equation and near surface air temperature as well as vapor pressure for sky emissivity in TSM and ATEB. In METRIC, $R_L\downarrow$ is estimated using T_s and atmospheric (sky) thermal emissivity (which is a function of atmospheric transmissivity for shortwave radiation). $R_L\uparrow$ is outgoing long wave radiation (W m^{-2}), and ε_o is broad-band surface thermal emissivity (dimensionless). The ε_o term was calculated using empirical equations developed by Tasumi et al. (2005) based on remote sensing LAI estimates [Eqn. (4)] and based on soil and vegetation

thermal spectral emissivities. The $(1- \varepsilon_o)R_L\downarrow$ term represents the fraction of incoming long wave radiation reflected from the surface, and $R_L\uparrow$ is the term that depends on broad band surface emissivity (function of biomass or leaf area index, LAI, presence) and T_s.

$$LAI = - \ln((0.69 – SAVI_{ID}) / 0.59) / 0.91 \quad (4)$$

where, $SAVI_{ID}$ is the Soil Adjusted Vegetation Index [(1 + L) (R-NIR) / (L + R+NIR)] calibrated for the soils of southern Idaho. It is an index that tries to remove soil background effects on vegetation indices. R is reflectance in the red band and NIR is reflectance in the near infrared band. L is a constant, equal to 1 for the soils of southern Idaho.

Soil heat flux (G) was modeled as a function of R_n, vegetation index, surface temperature, and surface albedo for near midday values (Bastiaanssen, 2000):

$$G = ((T_s – 273.15) (0.0038+0.0074 \alpha) (1-0.98 NDVI^4)) R_n \quad (5)$$

where, NDVI is the Normalized Difference Vegetation Index [(R-NIR)/(R+NIR)].

Sensible heat flux (H) is defined by the bulk aerodynamic resistance equation, which uses aerodynamic temperature (T_{aero}) and aerodynamic resistance to heat transfer (r_{ah}):

$$H = \rho_a Cp_a (T_{aero} – T_a) / r_{ah} \quad (6)$$

where, ρ_a is air density (kg m^{-3}), Cp_a is specific heat of dry air (1,004 J kg^{-1} K^{-1}), T_a is average air temperature, (K), T_{aero} is average aerodynamic temperature (K), which is defined for a uniform surface as the temperature at the height of the zero plane displacement (d, m) plus the roughness length (Z_{oh}, m) for sensible heat transfer, and r_{ah} is aerodynamic resistance (s m^{-1}) to heat transfer from Z_{oh} to Z_m [height of wind speed measurement (m)].

In the case of ATEB model, Chávez et al. (2005) linearly correlated inverted T_{aero} from measured H values by a network of eddy covariance (EC) systems to T_s (ºC) and LAI (m^2 m^{-2}) derived from airborne remote sensing data, and measured T_a (ºC) and horizontal wind speed (U, m s^{-1}) on corn and soybean fields in central Iowa.

$$T_{aero} = 0.534 T_s + 0.39 T_a + 0.224 LAI – 0.192 U + 1.67 \quad (7)$$

Eqn. (7) resulted with a coefficient of determination of 0.77. LAI was spatially estimated using the THP-specific LAI model (Gowda et al., 2007b). Equation (8) shows the LAI model.

$$LAI = 8.768 (NDVI)^{3.616} \quad (8)$$

In METRIC, H is estimated without needing to know T_a or T_{aero}, instead a temperature difference (dT), a function of T_s, was used as:

$$H = \rho_a Cp_a \frac{dT}{r_{ah}} \tag{9}$$

where, r_{ah} is calculated between two near surface heights, z_1 and z_2 (generally 0.1 and 2.0 m) using a wind speed extrapolated from some blending height above the ground surface (typically 100 to 200 m) and an iterative stability correction scheme for atmospheric heat transfer based on the Monin-Obhukov stability length scale (L_{MO}, similarity theory; Foken, 2006). In this study, a height of 200 m was used in the calculation of distributed friction velocity (u_*), a term utilized in the estimation of H.

Allen et al. (2007a) explained that dT (K) is a parameter that represents the near surface temperature difference between z_1 and z_2, and that the indexing of dT to T_s does not rely on absolute values of T_s, which allegedly reduces the error in calculating H substantially. Eqn. (10) characterizes the relationship of dT to T_s (Bastiaanssen, 1995).

$$dT = a + b\, T_s \tag{10}$$

where, *a* and *b* are empirically determined constants. The determination of *a* and *b* in Eqn. (10) involves locating a hot (dry) pixel in an agricultural field with large T_s and a cold (wet) pixel with a small T_s (typically one in an irrigated agricultural setting) in the remote sensing image. Once these pixels have been identified, the energy balance of Eqn. (1) can be solved for H_{cold} and H_{hot} as:

$$H_{cold} = (R_n - G)_{cold} - LE_{cold} \tag{11}$$

$$H_{hot} = (R_n - G)_{hot} - LE_{hot} \tag{12}$$

where, H_{hot} and H_{cold} are the sensible heat fluxes for the hot and cold pixels, respectively. The hot pixel is defined as having $LE_{hot} = 0$, i.e. no latent heat flux, which means that all available energy is partitioned to H. However, LE_{hot} may be non-zero and calculated according to a soil water budget if rainfall has occurred shortly before the image acquisition date. The cold pixel is assumed to have an LE value equal to 1.05 times that expected for a tall reference crop (i.e., alfalfa), thus LE_{cold} is set equal to 1.05 ET_r λ_{LE}, where ET_r is the hourly (or shorter time interval) tall reference (like alfalfa) ET calculated using the standardized ASCE Penman-Monteith equation. A 1.05 coefficient was used to estimate LE_{cold} as the cold pixels typically have an ET rate of 5% larger than that for the reference ET (ET_r) due to wet soil surface beneath a full vegetation canopy that will tend to increase the total ET rate (Allen et al., 2007a).

The hot pixel was chosen after careful screening of fallow/bare agricultural fields displaying high temperatures, high albedo, and low biomass (LAI). With the calculation of H_{hot} and $H_{cold,}$ Eqn. (9) was inverted to compute dT_{hot} and dT_{cold}. The '*a* and *b*' coefficients were then determined by fitting a line through the two pairs of values for dT and T_s from the hot and cold pixels. These *a* and *b* values were initial estimates that were

used in an Iterative stability Correction (ISC) scheme programmed in a spreadsheet. After some iterations, the ISC shows numerical convergence and the *a* and *b* coefficient, for each iteration, were then exported to a model in ERDAS Imagine to obtain the final stability corrected H image.

Instantaneous LE raster image values were obtained using Eqn. (1) and were converted in METRIC to an hourly evapotranspiration rate, ET_i in mm h^{-1}, by division by λ_{LE} and ρ_w as:

$$ET_i = 3600\ LE\ /\ \{[2.501 - 0.00236\ (T_s - 273.15)]\ (10^6)\ (1.0) \quad (13)$$

Reference ET fraction (ET_rF) is the ratio of ET_i to the reference ET_r that is computed from WS data at overpass time (hourly average). The WS information is explained in a subsequent section. Finally, the computation of daily or 24-h ET (ET_d), for each pixel, is performed as:

$$ET_d = ET_rF\ \ ET_r24 \quad (14)$$

where, ET_r24 is the cumulative 24-h ET_r for the day (mm d^{-1}).

For the calculation of ET_r and ET_r24 for alfalfa, weather data recorded by the USDA-ARS (Bushland) reference WS located on a grass field was used (TXHPET, 2006). The TXHPET reported hourly and daily weather data for the calculation of the grass (ET_o) and alfalfa (ET_r) reference ET by means of the standardized ASCE Penman-Monteith method (Allen et al., 2005b).

In the TSM, H is estimated by adding the H values of the soil background (H_{so}) and the crop canopy (H_c) that were estimated separately considering a vegetation-soil parallel resistance network, Norman et al. (1995).

$$H = H_c + H_{so} \quad (15)$$

$$H_c = \rho_a\ Cp_a\ (T_c - T_a)\ /\ r_{ah} \quad (16)$$

$$H_{so} = \rho_a\ Cp_a\ (T_{so} - T_a)\ /\ (r_{ah}\ r_{so}) \quad (17)$$

$$T_s = [f_c\ (T_c)^4 + (1 - f_c)\ (T_{so})^4]^{1/4} \quad (18)$$

where, T_c is canopy temperature, T_{so} is soil temperature, r_{so} is the resistance to heat flow above the soil (s m^{-1}), and f_c is fractional vegetation cover (function of LAI). An initial estimation of H_c applying Priestly and Taylor (1972) is found. Then, this H_c value is used to derive an initial T_c inverting Eqn. (16) assuming neutral atmospheric condition. Subsequently, Eqn. (18) is inverted and solved for T_{so} and updated values of H_c and H_{so} are computed correcting r_{ah} for atmospheric stability. T_c and T_{so} are verified by testing the estimated LE for a negative value, in which case temperatures are not correct, and the soil is assumed to have a dry surface. A new iteration cycle is needed, in which LE is set to zero for the soil component, and H_{so} is re-calculated ignoring LE. A new T_{so} and T_c values are found and sensible heat flux components are again estimated.

TSM and ATEB models estimate ET_d (mm d^{-1}) as follows:

$$ET_d = 86{,}400\ [EF\ (R_n - G)_d] / (\lambda_{LE}\ \rho_w) \quad (19)$$

$$EF = [LE / (R_n - G)]_i \quad (20)$$

where, 86,400 is the number of seconds in one day, EF is the evaporative fraction (dimensionless). λ_{LE} was calculated to be 2.45 MJ kg^{-1} (function of T_a), ρ_w as1.0 Mg m^{-3}. The subscripts "i" in Eqn. (20) and "d" in Eqn. (19) denote instantaneous and daily fluxes respectively.

ET Estimation Evaluation

Three different EB algorithms were evaluated by comparing their estimated ET values to lysimeter data. In addition, RS estimated R_n was compared with measured values on five lysimeters.

Results stemming from the comparison of spatially estimated ET and ET with lysimeters data were reported as absolute differences and in percent errors:

$$\text{Difference (\%)} = (ET\_p - ET\_L) \times 100 / ET_r \quad (21)$$

where, ET_p is the ET predicted and ET_L is the ET derived from water mass loss/gain data from lysimeters. ET_r is the alfalfa reference daily ET value acquired from the local Bushland-ARS weather station (TXHPET, 2006). A more comprehensive evaluation of ET estimation errors (comparison of estimated/measured ET) was carried out comparing 'mean bias error' (MBE) and 'root mean square error' (RMSE). These are the mean and standard deviation errors respectively.

Results and Discussion

Net Radiation Estimation

Remote sensing based R_n estimates resulted in larger bias for METRIC method. Its corresponding error was 56.8 ± 17.2 W m^{-2} (MBE ± RMSE) compared with 26.1 ± 10.9 W m^{-2} for the TSM, and 12.8 ± 7.4 W m^{-2} for the ATEB model. Figure 3 illustrates the comparison of three R_n estimates with measured values (Rn_m) in percent errors.

MBE for ATEB was 2.2% and was 7.6 % and 2.3 % lower than that for METRIC and TSM models. Standard deviation values of ATEB-estimated R_n were also small (1.3 %) compared to METRIC (3.1 %) and TSM (1.9 %). These results are an indication that using MODTRAN calibrated T_s and measured T_a and e, that it is possible to obtain more accurate spatially distributed R_n estimates.

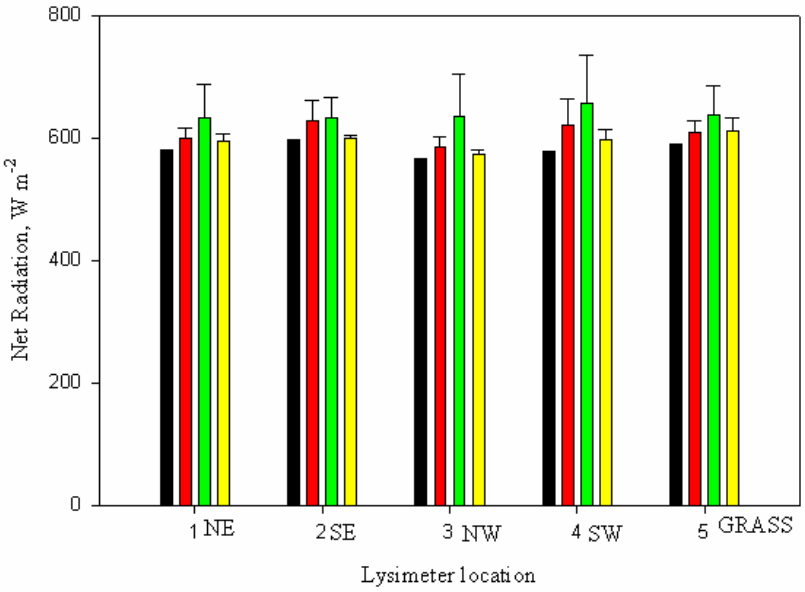

R_n	TSM	METRIC	ATEB
	%	%	%
MBE	4.5	9.8	2.2
RMSE	1.9	3.1	1.3

Figure 3. Net radiation estimates versus measured values showing error bars plus MBE and RMSE.

Overestimation of METRIC-based R_n compared to TSM or ATEB may be due to errors introduced in the computation of $R_{lw}\downarrow$ and $R_{lw}\uparrow$. In $R_{lw}\downarrow$ calculation, METRIC replaces T_a by T_s and estimates atmospheric (air) emissivity (ε_a) based on an estimation of atmospheric transmissivity that only uses ground elevation (respect to mean sea level) instead of T_a and actual vapor pressure, as in the Brutsaert (1975) model. In the Stefan-Boltzmann equation [$\varepsilon_a \sigma (T_a)^4$] used in the computation of $R_{lw}\downarrow$ if T_s is used instead of T_a ($T_s > T_a$ in our case), then a higher temperature will be raised to the power of 4 thus overestimating $R_{lw}\downarrow$ beyond the value that would have been estimated had T_a been used. The result is that adding $R_{lw}\downarrow$ to the shortwave net radiation [(1- α) R_s] yields a higher sum had the proper temperature been used.

Daily ET Estimation

Comparison of estimated ET_d values with lysimeter data indicated that ET estimated using ATEB gave smaller errors (-0.3 ± 0.7 mm d^{-1} or -3.2 ± 7.2 %) followed by that estimated using TSM (-0.8 ± 0.8 mm d^{-1} or -9.2 ± 9.0%) and METRIC (0.7 ± 0.9 mm d^{-1} or 7.4 ± 9.5 %). Graphical comparison to measured values (ETd_m) can be found in Fig. 4. ET prediction bias was larger for the NW Lysimeter irrespective of the method used for deriving surface temperature. It may be partly due to errors in the estimation of aerodynamic resistance and surface roughness length for the clumped grain sorghum in NW lysimeter field as none of these methods have been calibrated for clumped crops.

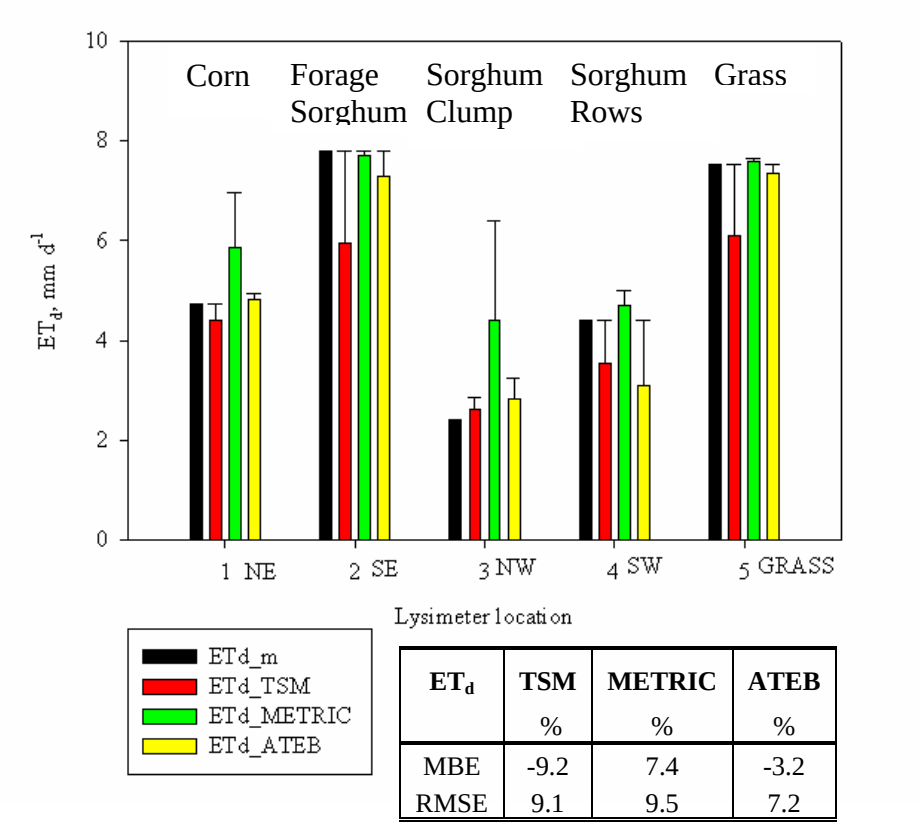

ET_d	TSM	METRIC	ATEB
	%	%	%
MBE	-9.2	7.4	-3.2
RMSE	9.1	9.5	7.2

Figure 4. ET_d estimates versus measured values showing error bars plus MBE and RMSE.

TSM estimated ET_d with absolute error of -20 and 16 % for SE and grass lysimeters fields, respectively. Higher absolute errors were partly due to the fact that both sorghum and grass fields were irrigated and had larger LAI values (4.2 and 3.0 m^2 m^{-2} respectively). It is possible that the TSM under predicted LE from the soil layer under closed canopy conditions (full cover). In addition, the grass lysimeter field is smaller than the thermal pixel size on the Landsat image and was contaminated by surrounded dry and irrigated fields. METRIC, on the other hand, showed overestimation errors of 12 to 22 % for NE and NW lysimeters fields. The NE lysimeter field was late planted to corn and showed a low LAI value of 0.4 m^2 m^{-2} while NW lysimeter field planted to clumped grain sorghum had an LAI value of 0.3 m^2 m^{-2}. It seems that the dT function may have not scaled H properly for high T_s areas, i.e. drier and sparse vegetation areas, due to lack of atmospheric corrections on the at sensor (satellite) surface brightness temperatures. In the case of ATEB, the only ET_d estimation error larger than 10 % occurred on the SW lysimeters field (-14.1 %). This field was planted to grain sorghum and had an LAI value of approximately 0.5 m^2 m^{-2}. Considering that the SW field was bound by fallow fields to the south and west and by natural vegetation (dryland) to the south-west, it is likely that local advection occurred in larger proportions to the SW lysimeters field, thus causing a larger error in ET_d estimation using ATEB. This model performance exceeded expectations since it was calibrated for a different region and under different environmental conditions.

Evidence of heat advection was proved by METRIC at the cold pixel heat flux estimation. H at the cold pixel was estimated as being -65.7 W m^{-2}; for an average wind speed of 3.0 m s^{-1} at overpass time. This negative H value represents an 11.2 % greater heat energy (on top of the available energy (R_n – G)) that was added from local/regional advected heat; thus resulting in an enhancement of ET in the same magnitude.

Figure 5 illustrates the spatial variability of daily ET in and around the lysimeter fields, where the difference between irrigated and dryland regimes for sorghum and corn crops is evident within the lysimeters fields (rectangle). Estimated ET_d values were varied from 7.8 mm d^{-1} for the irrigated silage sorghum field (SE lysimeters area) to 4.3 mm d^{-1} for grain sorghum (SW lysimeter area). Estimated ET_d for the grass lysimeter field was 7.6 mm d^{-1}. Greater ET_d rates, up to 9.9 mm d^{-1}, can be observed on the centre pivot-irrigated silage sorghum (field survey) belonging to the commercial Johnson Farm located on the west of the lysimeters fields. In addition, ET_d was 7.2 – 7.8 mm d^{-1} for the sub-surface drip irrigation (SDI) irrigated corn plots to the east of the lysimeters fields.

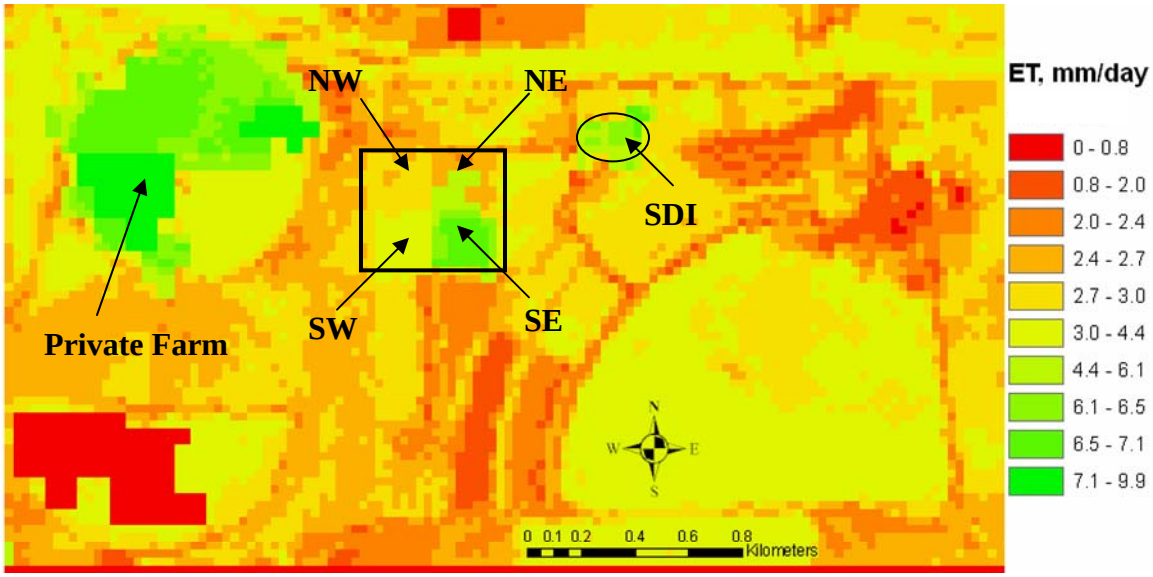

Figure 5. Spatially distributed daily ET on July 23, 2006 covering part of the USDA-ARS- CPRL and an adjoining private farm (centre pivots) to the west. SDI corn field shown by the oval polygon.

Conclusions

TSM, METRIC and ATEB algorithms were applied to the THP using a Landsat 5 TM image acquired on July 23, 2006 at 11:20 CST hours. Net radiation estimates using model ATEB more closely matched with measured values at lysimeters locations with MBE and RMSE values of 12.8 ± 7.4 W m^{-2} or 2.2 ± 1.3 % followed by the TSM (26.1 ± 10.9 W m^{-2} or 4.5 ± 1.9 %). METRIC showed a larger error of 56.8 ± 17.2 W m^{-2} (9.8 ± 3.1). METRIC's performance was most probably due to lack of atmospheric correction

on the thermal imagery and use of T_s in place of T_a in the estimation of the incoming long wave component of R_n.

Estimated ET_d compared well with lysimeter data. ET estimated using ATEB yielded the smallest estimation error (-0.3 ± 0.7 mm d^{-1} or -3.2 ± 7.2 %) followed by TSM (-0.8 ± 0.8 mm d^{-1} or -9.2 ± 9.0 %), while METRIC prediction error was 0.7 ± 0.9 mm d^{-1} (7.4 ± 9.5 %). TSM showed larger errors on lysimeter fields with LAI values larger than 3.0 m^2 m^{-2} indicating that it works better for sparse vegetation conditions where some soil background is detected by the remote sensing system, since this model partitions T_s into canopy and soil surface temperatures. Full canopy covers may prevent TSM from discriminating between canopy and soil surface conditions. METRIC showed larger prediction errors on low/dry biomass conditions, most likely due to lack of atmospheric correction for the thermal imagery which corrects hotter pixels in greater proportion than cooler pixels. Finally, ATEB underestimated ET by 14 % on the SW field perhaps due to local advection since this field was bounded by dry and fallow land.

In conclusion, all three tested models performed satisfactorily although, TSM and METRIC algorithms are more computational intense and require skilled users. The ATEB exceeded expectations since it was developed and tested for humid regions. However, a thorough evaluation and perhaps a local calibration of this type of model is needed for the THP.

References

ALLEN, R.G., TASUMI, M. and TREZZA, R., 2007, Satellite-based energy balance for Mapping evapotranspiration with internalized calibration (METRIC)-Model. *ASCE Journal of Irrigation and Drainage Engineering*, **133**(4), 380 - 394.

ALLEN, R.G., TASUMI, M. and TREZZA, R., 2005a, METRIC: Mapping evapotranspiration at high resolution – Applications manual for Landsat satellite imagery. University of Idaho. 130 p.

ALLEN, R.G., WALTER, I.A., ELLIOTT, R.L., HOWELL, T.A., ITENFISU, D., JENSEN, M.E. and SNYDER, R.L., 2005b., The ASCE Standardized Reference Evapotranspiration Equation. Report by the Task Committee on Standardization of Reference Evapotranspiration. ASCE, 0-7844-0805-X, 204 pp.

AXTELL, S., 2006, Ogallala Initiative. United States Department of Agriculture – Agricultural Research Service (USDA-ARS). Available online at: http://ogallala.tamu.edu. (Accessed November 20, 2006).

BASTIAANSSEN, W.G.M., 2000, SEBAL-based sensible and latent heat fluxes in the irrigated Gediz Basin, Turkey. *Journal of Hydrology*, **229**, 87 - 1000.

BASTIAANSSEN, W.G.M., MENENTI, M., FEDDES, R.A. and HOLTSLANG, A.A., 1998, A remote sensing surface energy balance algorithm for land (SEBAL): 1. Formulation. *Journal of Hydrology*, **212 - 213**, 198 - 212.

BASTIAANSSEN, W.G.M., 1995, Regionalization of surface flux densities and moisture indicators in composite terrain: A remote sensing approach under clear skies in Mediterranean climates. PhD dissertation, Wageningen Agricultural University, Wageningen, The Netherlands. CIP Data Koninklijke Blibliotheek, Den Haag.

BERK, A., ANDERSON, G.P., ACHARYA, P.K., CHETWYND, J.H., BERNSTEIN, L.S., SHETTLE, E.P., MATTHEW, M.W. and ADLER-GOLDEN, S.M., 2000, MODTRAN 4 User's Manual. Air Force Research Laboratory, Space Vehicle Directorate, Air Force Materiel Command, HANSCOM AFB, MA 01731-3010.

BREST, C.L. and GOWARD, S.N., 1987, Driving surface albedo measurements from narrow band satellite data. *International Journal of Remote Sensing*, **8**, 351 - 367.

BRUTSAERT, W., 1975, On a derivable formula for long-wave radiation from clear skies. *Water Resources Research*, **11**, 742 - 744.

CHANDER, G. and MARKHAM, B., 2003, Revised Landsat-5 TM radiometric calibration procedures and postcalibration dynamic ranges. *IEEE Transactions on Geoscience and Remote Sensing* **41**(11), 2674 - 2677.

CHÁVEZ, J.L., NEALE, C.M.U., HIPPS, L.E., PRUEGER, J.H. and KUSTAS, W.P., 2005, Comparing aircraft-based remotely sensed energy balance fluxes with eddy covariance tower data using heat flux source area functions. *Journal of Hydrometeorology*, **6**(6), 923 - 940.

CHEHBOUNI, A., SEEN, L.D., NJOKU, E.G., LHOMME, J.P., MONTENY, B. and KERR, Y.H., 1997, Estimation of sensible heat flux over sparsely vegetated surfaces. *Journal of Hydrology*, **188** – **189**, 855 – 868.

CHEHBOUNI, A., SEEN, L.D., NJOKU, J.P. AND MONTENY, B.A., 1996, Examination of the differences between radiative and aerodynamic surface temperatures over sparsely vegetated surfaces. *Remote Sensing of Environment*, **58**, 177 – 186.

CRAGO, R., FRIEDL, M., KUSTAS, W., and WANG, Y., 1999, Investigation of aerodynamic and radiometric land surface temperatures. NASA Scientific and Technical Aerospace Reports. Available on-line at: http://lshp.gsfc.nasa.gov/98-OES-11/crago/crago.html (accessed 10 June 2003).

Crago, R.D., 1998, Radiometric and equivalent isothermal surface temperatures. *Water Resources Research*, **34**(11), 3017– 3023.

DENNEHY, K.F., 2000, High Plains regional ground-water study: U.S. Geological Survey Fact Sheet 091-00, 6 p.

FOKEN, T., 2006, 50 Years of the Monin-Obukhov similarity theory. *Boundary-Layer Meteorology*, **119**(3), 431 - 447.

GOWDA, P.H., CHAVEZ, J.L., COLAIZZI, P.D., EVETT, S.R., HOWELL, T.A. and TOLK, J.A., 2007a, ET mapping for agricultural water management: Present status and challenges. *Irrigation Science*, DOI 10.1007/s00271-007-0088-6.

GOWDA, P.H., CHAVEZ, J.L., COLAIZZI, P.D., HOWELL, T.A., SCHWARTZ, R. AND MAREK, T.H., 2007b, Relationship between LAI and Landsat TM spectral vegetation indices in the Texas Panhandle. Paper number 072013. In *Proceedings of the 2007 ASABE Annual International Meeting*, Minneapolis, Minnesota, USA, 17 - 20 June 2007.

HOWELL, T.A., SCHNEIDER, A.D., DUSEK, D.A., MAREK, T.H. and STEINER, J.L., 1995, Calibration and scale performance of Bushland weighing lysimeters. *Transactions of the ASAE,* **38**, 1019 – 1024.

MCGUIRE, V.L., 2004, Water-level changes in the high plains aquifer, predevelopment to 2003 and 2002 to 2003. U.S. Geological Survey Fact Sheet FS-2004-3097. Available online at: http://pubs.usgs.gov/fs/2004/3097 (accessed December 8, 2006).

MCGUIRE, V.L., JOHNSON, M.R., SCHIEFFER, R.L., STANTON, J.S., SEBREE, S.K. and VERSTRAETEN, I.M., 2000, Water in storage and approaches to ground water management, high plains aquifer, 2000. U.S. Geological Survey Circular 1243.

NORMAN, J.M., KUSTAS, W.P. AND HUMES, K.S., 1995, A two-source approach for estimating soil and vegetation energy fluxes in observations of directional radiometric surface temperature. *Agricultural and Forest Meteorology*, **77**, 263 - 293.

SULEIMAN, A. AND CRAGO, R., 2004, Hourly and daytime evapotranspiration from grassland using radiometric surface temperatures. *Agronomy Journal*, **96**, 384 - 390.

SULEIMAN, A. AND CRAGO, R., 2002, Analytical land atmosphere radiometer model (ALARM) applied to a dense canopy. *Agricultural and Forest Meteorology,* **112**, 151 - 159.

TASUMI, M., TREZZA, R., ALLEN, R.G. AND WRIGHT, J.L., 2005, Operational aspects of satellite-based energy balance models for irrigated crops in the semi-arid U.S. *Journal of Irrigation and Drainage Systems,* **19**, 355 - 376.

TXHPET. 2006. Texas High Plains Evapotranspiration Network. Available online at: http://txhighplainset.tamu.edu/index.jsp (accessed September 4, 2006).